



IAU-ARAK

J. Iran. Chem. Res. 4 (2011) 263-279

Journal of the  
Iranian  
Chemical  
Research

www.iau-jicr.com

## Spectroscopic evidence of Cu(II) and Zn(II) complexes having amino acid based Schiff base: A special emphasis on *in vitro* antimicrobial, DNA binding and cleavage studies

Natarajan Raman \*, Abraham Selvan, Arunagiri Sakthivel

Research Department of Chemistry, VHNSN College, Virudhunagar-626 001, India

Received 1 May 2011; received in revised form 6 November 2011; accepted 6 November 2011

### Abstract

A new Schiff base ligand (L) obtained by the condensation reaction of N-acetylaceto-o-toluidine and 2-aminopropanoic acid (an amino acid), is used to synthesize four mononuclear complexes of [MLCl] and [ML<sub>2</sub>] types (where M = Cu(II) and Zn(II); L = Schiff base) by keeping the metal and ligand ratio as 1:1 and 1:2 respectively. This ligand and its complexes have been characterized on the basis of different spectral methods. EPR, UV-Vis. and magnetic moment data afford a square-planar geometry for the [MLCl] complexes and octahedral geometry for the [ML<sub>2</sub>] complexes. The observed low molar conductivity of these complexes at room temperature is consistent with their non-electrolytic nature. All the complexes display significant oxidative cleavage of circular plasmid pBR322 DNA in the presence of hydrogen peroxide. UV spectroscopic titration with CT DNA reveals that the complexes can bind to CT DNA and the binding constants to CT DNA have been calculated. The cyclic voltammograms of the complexes in the presence of CT DNA reveal that they bind to CT DNA probably by the intercalative binding mode. The antimicrobial activity of the complexes has been tested against microorganisms showing that they exhibit higher activity than free Schiff base ligand.

**Keywords:** DNA binding; Antimicrobial activity; 2-aminopropanoic acid; Schiff base complexes.

### 1. Introduction

Active and well defined Schiff base ligands are considered as 'privileged ligands' because they are easily prepared by the condensation reaction of aldehydes or ketones with amines and are able to stabilize different metals in various oxidation states [1]. Schiff base complexes are extensively studied due to synthetic flexibility, selectivity and sensitivity towards variety of metal ions [2]. Considerable attention has been given to the preparation of transition metal complexes of Schiff bases derived from amino acids due to their biological importance [3]. In the recent years, there has been considerable interest in the chemistry of tridentate transition metal complexes of Schiff bases. Tridentate Schiff base ligands involving N, O donor sites possess many advantages such as facile approach for synthesis, relative tolerance, readily

\* Corresponding author. Tel.: +091-92451-65958, fax: +09-4562-281338.  
E-mail address: drn\_raman@yahoo.co.in (N. Raman)

adjusted ancillary ligands, and tunable steric and electronic coordination environments on the metal centre. The transition metals, zinc and copper are some of the most frequently occurring elements integrated into essential biochemical pathways. Various transition metal complexes with bi-, tri- and tetradentate Schiff bases containing nitrogen and oxygen donor atoms play important role in biological systems and represent interesting models for metalloenzymes, which efficiently catalyze the reduction of dinitrogen and dioxygen [4]. In addition, complexes of amino acid Schiff bases are considered to constitute new kinds of potential antibacterial and anticancer reagents [5].

Transition metal complexes that cleave DNA under physiological condition are of current interest in the development of artificial nucleases [6]. Most studies of nucleic acid cleavage by the small molecules have been focused on oxidative cleavage and photocleavage [7]. However, these oxidative cleavage agents require the addition of an external agent (light, oxidative and/or reductive agent) to initiate cleavage. Among several types of transition metal complexes used as hydrolytic cleavage agents, copper(II) complexes have attracted special attention, which has been observed as cofactor in many nucleases[8]. In this connection, we have prepared four new transition metal complexes by changing the stoichiometry of the metal to ligand ratio and investigated their DNA binding activity.

The aim of the present work is to insert NO group in amino acid Schiff bases. As we know amino acid Schiff bases readily form complexes with metal ions which play an important role as the basic compounds for modeling more complicated amino acid Schiff bases [9]. In our study on coordination chemistry of amino acid Schiff bases, we thought that it would be useful to synthesize coordination compounds of a Schiff base containing azomethine moieties and to evaluate them for their antimicrobial activities. Bearing the above facts in our mind, in the present work, we wish to report the synthesis, structure, redox properties, anti-biogram and DNA binding and cleavage studies of transition metal complexes of amino acid Schiff base derivative. A comparative antibacterial and antifungal activity of these compounds is evaluated.

## **2. Experimental**

### *2.1. Reagents and equipments*

CT DNA, gel loading buffer, Tris base, N-acetylaceto-o-toluidine and 2-aminopropanoic acid were purchased from Sigma–Aldrich. Ethidium bromide (EB), calf thymus DNA (CT DNA) and pBR322 plasmid DNA were also purchased from Sigma. All reagents and chemicals were procured from Merck (Darmstadt, Germany). Solvents used for electrochemical and spectroscopic studies were purified by standard procedures [10].

All the experiments involved in the interaction of the ligand and its metal complexes with CT DNA were carried out in doubly distilled water buffer containing 5 mM Tris [Tris(hydroxymethyl)-aminomethane] and 50 mM NaCl and adjusted to pH 7.2 with hydrochloric acid. Solution of CT DNA in Tris–HCl buffer gave ratio of UV absorbance of about 1.8–1.9:1 at 260 and 280 nm, indicating that the CT DNA was sufficiently free of protein [11]. The CT DNA concentration per nucleotide was determined spectrophotometrically by employing an extinction coefficient of  $6600 \text{ M}^{-1} \text{ cm}^{-1}$  at 260 nm [12].

UV–Vis spectra were recorded on a Shimadzu Model 1601 UV-Visible Spectrophotometer. IR spectra were recorded (KBr) with a Perkin-Elmer FTIR-1605 spectrophotometer.  $^1\text{H}$  NMR spectra were taken at room temperature on a Varian XL-300 MHz spectrometer with tetramethylsilane (TMS) as the internal standard. Microanalyses were carried out on a PerkinElmer 240 elemental analyzer. Fast atom bombardment mass spectra (FAB-MS) were obtained in a 3-nitrobenzyl alcohol matrix using a VGZAB-HS spectrometer. The X-band EPR spectra of the complexes were recorded at RT (300 K) and LNT (77 K) using TCNE as the g-marker. Room temperature magnetic susceptibility measurements were carried out on a modified

Gouy-type magnetic balance, Hertz SG8-5HJ. The molar conductivity of the complexes in DMF solution ( $10^{-3}$  M) was measured using a conductometer model 601/602.

## 2.2. Pharmacology

### 2.2.1. In vitro antibacterial and antifungal assay

The antibacterial and antifungal activity of freshly synthesized complexes in DMF was tested against the Gram-positive bacteria *Staphylococcus aureus*, *Bacillus subtilis*, the Gram-negative bacteria *Escherichia coli*, *Salmonella typhi*, and against the fungi *Aspergillus niger*, *Aspergillus flavus*, *Candida albicans*, and *Rhizoctonia bataicola*. The activity was then compared with some reference antibiotics that were purchased from the market. All the complexes and the parent ligand were screened for their activity against the test organisms. The filter paper disc agar diffusion method was adopted for the activity measurements [13]. The bacterial strains were grown in nutrient agar slants and the fungal strains were grown in Sabouraud dextrose agar slants. The viable bacterial cells were swabbed onto nutrient agar plates and the fungal spores onto Sabouraud dextrose agar plates. The compounds were dissolved in DMF to a final concentration of 0.1%. A medium inoculated with the respective cultures and the test solutions of the compounds in different concentrations for bacterial cultures and for fungal cultures were allowed to stay in the disc. The petri plates were incubated for 36 h for bacterial cultures and 72 h for fungal cultures. All the compounds were screened against nystatin as reference for fungal cultures and streptomycin for bacterial cultures in their standard concentration of 200  $\mu\text{g}/\text{disc}$ , then the growth of microorganisms was observed. When no growth of microorganisms was observed in the medium containing the lowest concentration of test materials, the MIC of the test material was defined at this point of dilution. The MIC was measured to be the lowest concentration after the period of incubation. The solvent, DMF used for the preparation of compounds did not show any inhibition against the tested microorganisms.

### 2.2.2. Assay of nuclease activity

The DNA cleavage activity of the Schiff base metal complexes was monitored by agarose gel electrophoresis on pBR322 DNA. The tests were performed under aerobic conditions with  $\text{H}_2\text{O}_2$  as an oxidant. The metal complexes were dissolved in 50 mM Tris-HCl/5 mM NaCl buffer (pH 7.2). For DNA cleavage studies, the reactions were carried out under illuminated conditions using UV source at 365 nm (12 W). A concentration of the metal complexes (25  $\mu\text{M}$ ) was taken in clean eppendorf tubes, 50  $\mu\text{M}$  of hydrogen peroxide and pBR322 DNA (1  $\mu\text{L}$  of 0.10  $\mu\text{g}/\text{mL}$ ) was added. The contents were incubated at 37  $^\circ\text{C}$  for 2 h and loaded on 1% agarose gel after mixing 5  $\mu\text{L}$  of loading buffer (25% bromophenol, 30% glycerol (3  $\mu\text{L}$ ) and 0.25% xylene cyanol). The electrophoresis was carried out for 1.5 h at 60 V in TAE buffer. After electrophoresis, the gel was stained with 1  $\mu\text{g}/\text{cm}^3$  EB for 30 min prior to being photographed under UV light. Due corrections were made for the lower level of nicked circular (NC) form present in the original supercoiled (SC) DNA sample and for the lower affinity of EB binding to SC compared to NC and linear forms of DNA [14].

### 2.2.3. Viscosity experiment

Viscosity measurements were carried out using an Ubbelodhe viscometer, immersed in a thermostatic water-bath that maintained at a constant temperature at  $25.0 \pm 0.1$   $^\circ\text{C}$ . The compounds (1–10  $\mu\text{M}$ ) were titrated into the CT-DNA solution (10  $\mu\text{M}$ ) which presented in the viscometer. The flow time of each sample was measured by a digital stop-watch for three times, and an average one was calculated. Data are presented as  $(\eta/\eta^0)^{1/3}$  vs. binding ratio [15], where  $\eta$  and  $\eta^0$  are the viscosity of DNA in the presence and absence of complex, respectively.

### 2.3. Synthesis of ligand and its metal complexes

The Schiff base ligand and its [MLCl] (1 and 2) and [ML<sub>2</sub>] (3 and 4) complexes were prepared as follows: An ethanolic solution (20 mL) of N-acetylaceto-o-toluidine (1.91 g, 10 mmol) was stirred for *ca.* 2 h with an ethanolic solution of 2-aminopropanoic acid (0.9 g, 10 mmol) in alkaline medium (0.44 g of NaOH, 11 mmol) and the mixture was refluxed for *ca.* 3h. The resulting solution was evaporated under room temperature. The solid product (L = N-(2-methylphenyl)-3-(2'-iminesodiumpropanate)-butanamide) filtered-off, washed several times with ether and then recrystallised from ethanol.

The aqueous solution of Schiff base (L) (0.284 g, 1 mmol) was refluxed for *ca.* 4 h with an aqueous solution of the copper(II) chloride (1)/zinc(II) chloride (2) (0.170 g/0.136 g, 1 mmol). The solid product of the 1:1 (metal:ligand ratio) complexes [*i.e.*(1) / (2)] was separated. It was filtered and washed with ethanol and dried *in vacuo*.

The aqueous solution of Schiff base L (0.57 g, 2 mmol) was refluxed for *ca.* 4 h with an aqueous solution of the copper(II) chloride (3)/zinc(II) chloride (4) (0.170 g/0.136 g, 1mmol). The solid product of the 1:2 (metal:ligand ratio) complexes [*i.e.* (3) / (4)] was separated. It was filtered and washed with ethanol and dried *in vacuo*.

### 3. Results and discussion

The synthesized ligand and its Cu(II) and Zn(II) complexes are air stable. They are soluble in water and sparingly soluble in common organic solvents. They have been characterized by the analytical and spectral techniques. The physical characterization, microanalytical, molar conductance and magnetic susceptibility data of the compounds are given in Table.1. Molar conductivity of the ligand in water is found to be high which indicates that 1:1 electrolytic nature of the ligand which confirms the fact that the ligand is present in the form of its sodium salt. The observed low molar conductivity of the complexes in water at room temperature is consistent with the non-electrolytic nature of the complexes.

**Table 1**

Physical characterization, analytical, molar conductance and magnetic susceptibility data of the ligand and its complexes

Compound	Colour	Empirical formula	Yield (%)	Found (Caclcd) (%)				Molar Conductance ( $\Lambda_m$ ) (ohm <sup>-1</sup> cm <sup>2</sup> mol <sup>-1</sup> )	$\mu_{\text{eff}}$ (BM)
				M	C	H	N		
Ligand	Yellow	C <sub>14</sub> H <sub>17</sub> N <sub>2</sub> O <sub>3</sub> Na	68	----	58.8 (59.1)	5.7 (6.0)	9.7 (9.9)	48.2	----
[CuLCl]	Blue	[CuC <sub>14</sub> H <sub>17</sub> N <sub>2</sub> O <sub>3</sub> Cl]	49	17.2 (17.6)	46.4 (46.7)	4.5 (4.8)	7.8 (7.9)	9.5	1.89
[ZnLCl]	Dirty white	[ZnC <sub>14</sub> H <sub>17</sub> N <sub>2</sub> O <sub>3</sub> Cl]	43	17.8 (18.1)	46.0 (46.4)	4.5 (4.7)	7.4 (7.7)	3.7	----
[CuL <sub>2</sub> ]	Blue	[CuC <sub>28</sub> H <sub>34</sub> N <sub>4</sub> O <sub>6</sub> ]	53	10.6 (10.8)	57.0 (57.4)	5.5 (5.9)	9.3 (9.6)	7.5	1.96
[ZnL <sub>2</sub> ]	Dirty white	[ZnC <sub>28</sub> H <sub>34</sub> N <sub>4</sub> O <sub>6</sub> ]	47	10.8 (11.1)	56.8 (57.2)	5.4 (5.8)	9.1 (9.5)	10.4	----

#### 3.1. IR spectra

The IR bands observed at 1700-1690 and 1640-1630 cm<sup>-1</sup> due to  $\nu_{\text{C=O}}$  and  $\nu_{\text{C=N}}$  stretching frequencies respectively in the free ligand are shifted towards lower values in all complexes

(1685-1670 and 1620-1600  $\text{cm}^{-1}$ ) indicating that the carbonyl oxygen atom of the N-acetylaceto-o-toluidine residue and the azomethine nitrogen atom are coordinated to the metal ion. The  $\nu_{\text{asym}}(\text{COO}^-)$  band of free ligand observed at 1610-1590  $\text{cm}^{-1}$  is shifted to lower wave number in the spectra of metal complexes i.e.  $\sim 1574 \text{ cm}^{-1}$ . The  $\nu_{\text{sym}}(\text{COO}^-)$  band of free ligand observed at 1400  $\text{cm}^{-1}$  is shifted to lower wave number in the spectra of metal complexes i.e.  $\sim 1378 \text{ cm}^{-1}$ , representing coordination of carboxylic acid group with metal ion through the oxygen atom [16]. For the copper complex (1), the bands appeared in the low frequency regions at 384  $\text{cm}^{-1}$ , 461  $\text{cm}^{-1}$  and 428  $\text{cm}^{-1}$  are characteristic to M-Cl, M-O and M-N stretching vibrations, respectively, that are not observed in the spectrum of free ligand and the new peaks of copper complex (3) observed in the regions at 459  $\text{cm}^{-1}$  and 419  $\text{cm}^{-1}$  are assigned to the characteristic bands of M-O and M-N respectively, which are not observed in the free ligand [17,18].

### 3.2. Magnetic moment and electronic absorption spectra

The electronic spectral data along with magnetic susceptibility measurements gave adequate support in establishing the geometry of the metal complexes. In the electronic spectra of the ligand and its mononuclear metal complexes, the wide range bands have been observed due to either the  $\pi \rightarrow \pi^*$  and  $n \rightarrow \pi^*$  of C=N chromophore or charge-transfer transition arising from  $\pi$  electron interactions between the metal and ligand, which involves either a metal-to-ligand or ligand-to-metal electron transfer [19,20]. The absorption bands between 45,914 and 33,898  $\text{cm}^{-1}$  in free ligand change a bit in intensity for metal complexes. The absorption shift and intensity change in the spectra of the metal complexes are most likely originated from the metalation which increases the conjugation and delocalization of the whole electronic system and results in the energy change of  $\pi \rightarrow \pi^*$  and  $n \rightarrow \pi^*$  transition of the conjugated chromophore [21].

The copper complexes (1) and (3) are magnetically normal with magnetic moment of 1.89 and 1.96 B.M respectively. The copper complex (1) shows d-d transitions nearly at 15,971 and 15,408  $\text{cm}^{-1}$  which can be assigned to  ${}^2B_{1g} \rightarrow {}^2A_{1g}$  and  ${}^2B_{1g} \rightarrow {}^2E_g$  transitions respectively, revealing that the copper(II) complex exists in square-planar geometry [22]. In complex (3), the observed band at 12,239  $\text{cm}^{-1}$ , assigned to  ${}^2E_g \rightarrow {}^2T_{2g}$  transition, reveals a distorted octahedral geometry around the central copper ion. Electronic absorption spectra of the complexes (1) and (3) are shown in Fig. S1 (supplementary material). The absorption regions, assignment and the proposed geometry of the ligand and its complexes are given in Table 2.

The zinc(II) complexes are found to be diamagnetic. By analogy with those described for the complexes containing N, O donor Schiff bases, the electronic spectral data and empirical formulae of the zinc(II) complexes are consistent with a tetrahedral geometry around the metal ion [23].

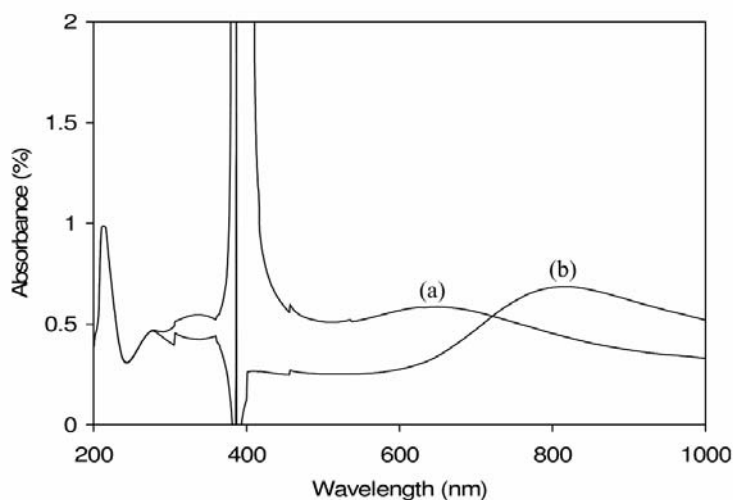


**Fig. S1.** Electronic absorption spectra of: a) complex 1 and b) complex 3

**Table 2**

Electronic absorption spectral data of the ligand and its Cu(II) and Zn(II) metal complexes

Compound	Absorption (cm <sup>-1</sup> )	Band Assignment	Geometry
L	45914	INCT	----
	37037	INCT	
	33898	INCT	
(1)	35335	INCT	Square-planar
	46948	INCT	
	15971	<sup>2</sup> B <sub>1g</sub> → <sup>2</sup> A <sub>1g</sub>	
	15408	<sup>2</sup> B <sub>1g</sub> → <sup>2</sup> E <sub>g</sub>	
(2)	35714	INCT	----
	46969	INCT	
(3)	34722	INCT	Distorted octahedral
	47373	INCT	
	21882	INCT	
	12239	<sup>2</sup> E <sub>g</sub> → <sup>2</sup> T <sub>2g</sub>	
(4)	35846	INCT	----
	47569	INCT	

### 3.3. <sup>1</sup>H NMR spectra

<sup>1</sup>H NMR spectra of Schiff base and its zinc complex (2 and 4) were recorded in CDCl<sub>3</sub>. They show a group of multiple signals corresponding to the aromatic protons at 6.9–7.4 ppm. The three signals of the Schiff base and its zinc complexes around ~2.6, ~2.3 and ~2.1 ppm are assigned to –CH<sub>3</sub>, –CH<sub>2</sub>– and –CH protons respectively.

For zinc complex **2**, the aromatic protons were observed as multiplets in the aromatic region 6.90–6.79 ppm. The aliphatic –CH<sub>2</sub> and –CH<sub>3</sub> protons were observed as a singlet at 2.52 and 2.36 ppm, respectively. The spectrum of the Schiff base exhibits signal at 8.9 ppm, attributed to –NPh proton. The absence of –COOH peak in the ligand confirms that the ligand is in the form of its sodium salt. The –NPh peak of the zinc complexes is not affected compared to the free ligand, suggesting that the –NH nitrogen is not taking part in complexation with metal ion.

### 3.4. FAB-Mass spectra

The mass spectrum of the studied compound is characterized by moderate to high relative intensity molecular ion peaks. It is obvious that the molecular ion peaks are in good agreement with their suggested empirical formulae as indicated from elemental analyses. FAB Mass spectrum of the ligand shows a molecular ion peak (M+1) at m/z 285 corresponding to [C<sub>14</sub>H<sub>17</sub>N<sub>2</sub>O<sub>3</sub>Na]<sup>+</sup> ion. Its complexes **1** and **3** show the molecular ion (M+1) peaks at m/z = 361 and 588, which confirm the stoichiometry as being of [MLCl] and [ML<sub>2</sub>] type respectively. The FAB mass spectra of **2** and **4** show a molecular ion (M<sup>+</sup>) peak at m/z = 362 and 589 respectively, which suggests the stoichiometry of the complexes and confirms the proposed formula. The spectrum of **2** also exhibits two additional peaks m/z at 363 and 364, which are corresponding to (M+1) and (M+2) peaks respectively. The mass spectra of the ligand and its copper complexes are shown in Fig. S2 and Fig. S3 (supplementary material) respectively.

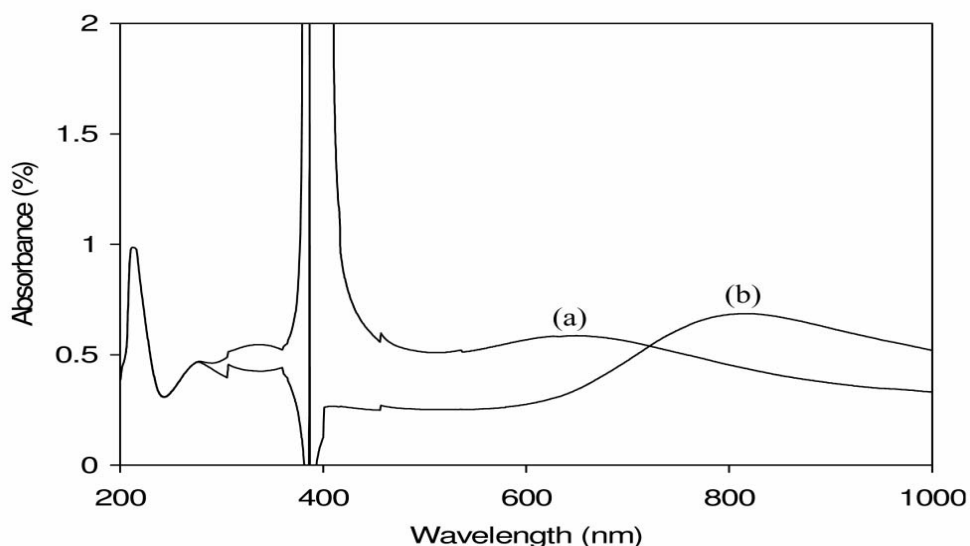


Fig. S2. FAB-Mass spectrum of Ligand.

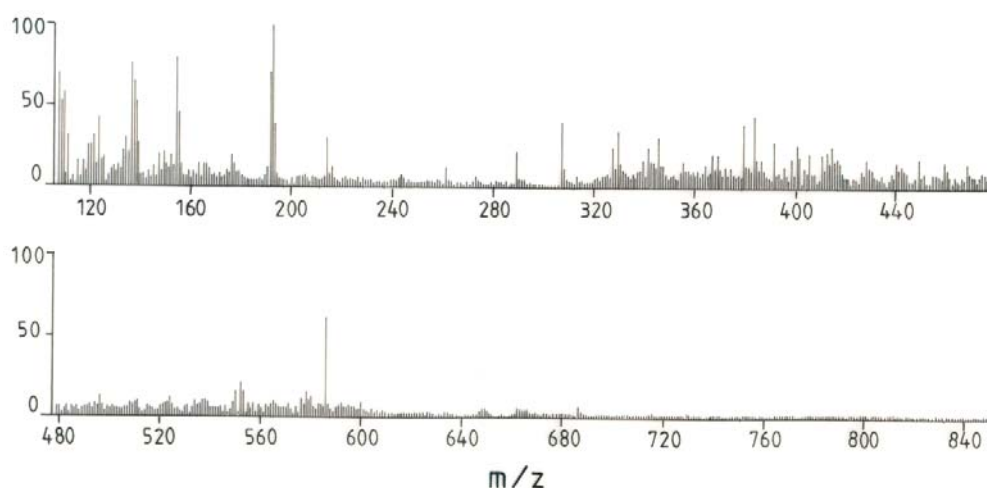


Fig. S3. FAB-Mass spectrum of complex 3.

### 3.5. EPR spectra

The X-band EPR spectrum of complex 1 was recorded in DMSO solution at 300 and 77 K. From the observed values, ( $A_{\parallel} = 147 > A_{\perp} = 58$ ;  $g_{\parallel} = 2.29 > g_{\perp} = 2.06 > 2.0027$ ), it is clear that the EPR parameters of the complex coincide well with related systems which suggest that the complex has square-planar geometry and the system is axially symmetric [24]. This is also supported by the fact that the unpaired electron lies predominantly in the  $d_{x^2-y^2}$  orbital. In the axial spectra the  $g$ -values are related with exchange interaction coupling constant ( $G$ ) by the expression,  $G = g_{\parallel} - 2.0027/g_{\perp} - 2.0027$ . According to the Hathaway [25], if the  $G$  value is larger than four, the exchange interaction is negligible because the local tetragonal axes are aligned parallel or slightly misaligned. If the value of  $G$  is less than four, the exchange interaction is considerable and the local tetragonal axes are misaligned. For the present copper complex, the  $G$  value is 4.9 which suggests that the local tetragonal axes are aligned parallel or slightly misaligned and consistent with a  $d_{x^2-y^2}$  ground state. The in-plane  $\sigma$ -bonding covalency parameter,  $\alpha^2$  is related to  $A_{\parallel}$ ,  $g_{\parallel}$  and  $g_{\perp}$  according to the following equation:

$$\alpha^2 = (A_{\parallel}/P) + (g_{\parallel}-2.0027) + 3/7(g_{\perp} - 2.0027) + 0.04$$

If the  $\alpha^2$  value = 0.5, it indicates complete covalent bonding, while the value of  $\alpha^2 = 1.0$  suggests complete ionic bonding. The observed value of  $\alpha^2$  (0.7) indicates that the complexes have some covalent character. The out-of-plane  $\pi$  bonding ( $\gamma^2$ ) and in plane  $\pi$ -bonding ( $\beta^2$ ) parameters are calculated from the following expressions:

$$\beta^2 = (g_{\parallel} - 2.0027) E / (-8\lambda\alpha^2)$$

$$\gamma^2 = (g_{\perp} - 2.0027) E / (-2\lambda\alpha^2)$$

In these equations,  $\lambda = -828 \text{ cm}^{-1}$  for the free metal ion and  $E = 15,971 \text{ cm}^{-1}$ . The observed  $\beta^2$  (1.19) and  $\alpha^2$  (0.76) values indicate that there is interaction in the out-of-plane  $\pi$ -bonding whereas the in-plane  $\pi$ -bonding is completely covalent. This is also confirmed by orbital reduction factors, which are estimated using the relations,  $K_{\parallel} = (g_{\parallel} - 2.0027)(\Delta E / -8\lambda)$  and  $K_{\perp} = (g_{\perp} - 2.0027)(\Delta E / -8\lambda)$ . Significant information about the nature of bonding in the copper(II) complex can be derived from the relative magnitudes of  $K_{\parallel}$  and  $K_{\perp}$ . In the case of pure  $\sigma$ -bonding  $K_{\parallel} \approx K_{\perp} = 0.77$ , whereas  $K_{\parallel} < K_{\perp}$  implies considerable in-plane  $\pi$ -bonding while for out-of-plane  $\pi$ -bonding  $K_{\parallel} > K_{\perp}$ . For the present complex, the observed order is  $K_{\parallel}$  (0.96)  $>$   $K_{\perp}$  (0.42) implying a greater contribution from out-of-plane  $\pi$ -bonding than from in-plane  $\pi$ -bonding in metal-ligand  $\pi$ -bonding. EPR spectrum of the copper complex 3 recorded in polycrystalline state at room temperature provides information about the coordination environment around Cu(II) in the complex which is presented in Fig. S4 (supplementary material). The EPR parameters of the complex 3 are  $g_{\parallel}$  (2.18),  $g_{\perp}$  (2.03),  $g_{av}$  (2.11),  $A_{\parallel}$  (185) and  $A_{\perp}$  (35) and the energies of the d-d transitions were used to evaluate the bonding parameters  $\alpha^2$ ,  $\beta^2$  and  $\gamma^2$  which may be regarded as measurement of covalency of the in-plane  $\sigma$ -bonding, in-plane  $\pi$ -bonding and out of plane  $\pi$ -bonding respectively. The trend exhibits an auxiliary symmetric g-tensor parameters with  $g_{\parallel} > g_{\perp} > 2.0027$  indicating that the copper site has a  $d_{x^2-y^2}$  ground state characteristic of octahedral geometry [25]. The observed values of  $\alpha^2$  (0.74) and  $\beta^2$  (0.59) parameters indicate that the complexes have some covalent character and there is interaction in the out-of-plane  $\pi$ -bonding.

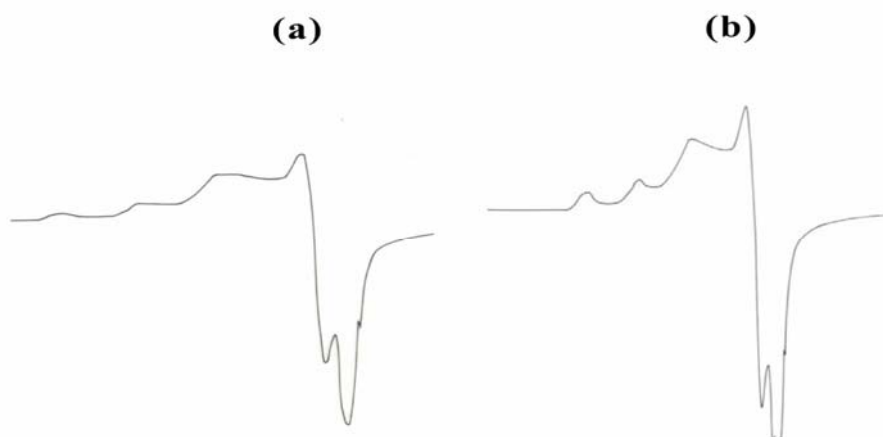


**Fig. S4.** EPR spectra of the copper complex 3 (a) at 300 K and (b) 77 K in DMSO solution

### 3.6. Proposed structure of complexes

Based on above studies, a four coordinated square-planar geometry and six coordinated octahedral geometry have been proposed for the  $[MLX]$  and  $[ML_2]$  complexes which are shown in Fig. 1 and Fig. 2.

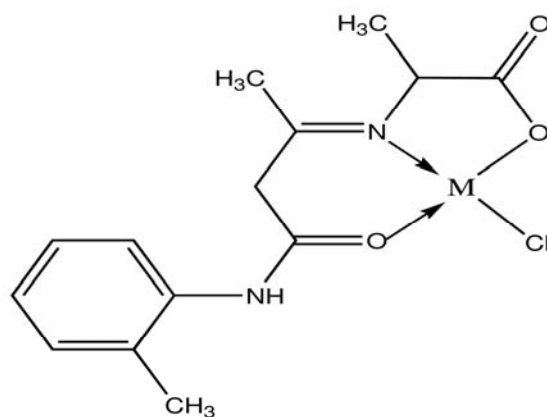


**Fig. 1.** Structure of complexes 1 and 2, where, M = Cu(II) /Zn(II) [1:1 (M:L) molar ratio].

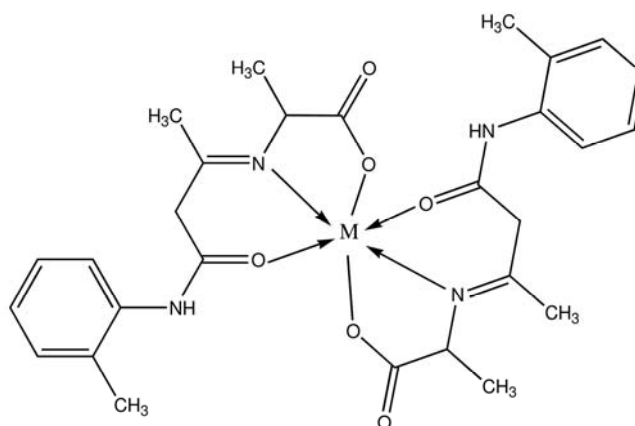


**Fig. 2.** Structure of complexes 3 and 4, where, M = Cu(II) /Zn(II) [1:2 (M:L) molar ratio].

### 3.7. DNA-binding experiment

In these studies, all the compounds were dissolved in a mixed solvent of 1% DMF and 99% Tris-HCl buffer (5 mM Tris-HCl, 50 mM NaCl, pH 7.2) at a concentration of  $1.0 \times 10^{-3}$  M. All the experiments involving the interaction of complexes with CT-DNA were carried out in Tris-HCl buffer.

#### 3.7.1. DNA binding analysis using electronic spectral method

The application of electronic absorption spectroscopy in DNA-binding studies is one of the most effective techniques [26]. The absorption spectra of the metal complexes in the absence and presence of CT-DNA are given in Fig. 3. The absorption spectral titration of the complexes 1-4 with CT-DNA was followed by monitoring the MLCT bands of the metal complexes. Absorption titration experiment was performed with fixed concentrations of the compounds (25  $\mu$ M), while gradually increasing concentration of DNA. On increasing the CT-DNA concentration, the hypochromism was found to increase with a red shift (bathochromic shift) in the UV band of the complexes [27, 28]. In order to compare quantitatively the binding strength of the metal complexes, the intrinsic binding constants  $K_b$  of the complexes with DNA were obtained by monitoring the changes in absorbance with increasing concentration of DNA using the following equation:

$$[\text{DNA}] / (\epsilon_a - \epsilon_f) = [\text{DNA}] / (\epsilon_b - \epsilon_f) + 1 / [K_b(\epsilon_b - \epsilon_f)]$$

Where [DNA] is the concentration of DNA in base pairs, the apparent absorption coefficient  $\epsilon_a$ ,  $\epsilon_f$  and  $\epsilon_b$  correspond to  $A_{\text{obs}}/[\text{complex}]$ , the extinction coefficient for the free complexes and the extinction coefficient for the free complexes in the fully bound form, respectively. The magnitude of the binding strength of compounds with CT DNA can be estimated through the binding constant  $K_b$ , which can be obtained by monitoring the changes in the absorbance at the corresponding  $\lambda_{\text{max}}$  with increasing concentrations of CT DNA. In plots of  $[\text{DNA}] / (\epsilon_a - \epsilon_f)$  versus  $[\text{DNA}]$ ,  $K_b$  is given by the ratio of slope to the intercept [29]. The  $K_b$  values of metal(II) complexes thus obtained with different hypochromicity of coordinated copper(II) and zinc(II) chelates are shown in Table 3.

Upon the addition of CT-DNA, notable hypochromic effect was observed. The hypochromic effect, characteristic of intercalation has been usually attributed to the interaction between the electronic states of the compound chromophores and those of the DNA bases [30]. Thus, the spectroscopic changes suggested that all of the compounds, especially the complexes had strong interaction with DNA.

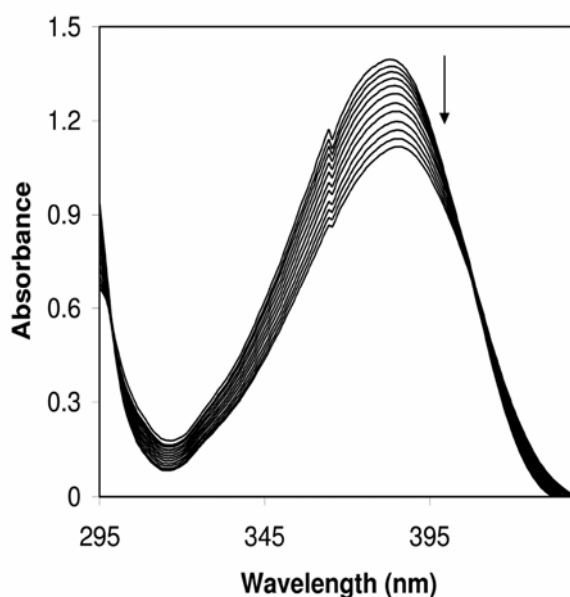


**Fig. 3.** Absorption spectra of complex 3 in presence of DNA in Tris-HCl buffer upon addition of CT DNA; [complex] = 25  $\mu\text{M}$ . Arrow shows the absorbance changing upon the increase of DNA concentration.

**Table 3**

Absorption spectral properties of synthesized metal complexes in presence of CT DNA

Complexes	$\lambda_{\text{max}}$ (nm)		$\Delta\lambda$ (nm)	%H	$K_b \times 10^3$ ( $\text{M}^{-1}$ )
	Free	Bound			
1	328.0	330.6	2.6	10	1.1
2	320.0	321.0	1.0	6	0.4
3	325.5	326.8	1.3	8	0.6
4	322.6	323.8	1.2	9	0.5

## 3.7.2. DNA binding analysis using cyclic voltammogram method

Typical CV curves for  $1.0 \times 10^{-3}$  mol dm<sup>-3</sup> of copper complexes in Tris-HCl buffer (pH 7.2) in the absence and presence of different concentration of DNA are shown in Fig. S5 (supplementary material). The electrochemical data are given in Table 4. All the copper complexes show one well-defined redox couple corresponding to Cu(II)/Cu(I), as expected. In the absence of DNA, cathodic peak appears in the range of 0.140 –0.525 V corresponds to the one electron reduction of copper(II) and the corresponding anodic peak appears in the 0.408–0.630 mV positive potential region. The measured  $\Delta E_p$  values (0.125-0.132 V) clearly indicate that these redox couples are quasi-reversible. The  $i_{pa}/i_{pc}$  falls at less than unity, clearly confirming one electron transfer in this redox process. In the incremental addition of CT DNA to the complex, the redox couples cause a negative shift in  $E_{1/2}$  and a decrease in  $\Delta E_p$ . The  $i_{pa}/i_{pc}$  values also decrease in the presence of DNA. The decrease of the anodic and cathodic peak currents of the complex in the presence of DNA is due to decrease in the apparent diffusion coefficient of the copper(II) complex upon complexation with the DNA macromolecule. These results show that copper(II) complex stabilizes the duplex (GC pairs) by intercalating way.

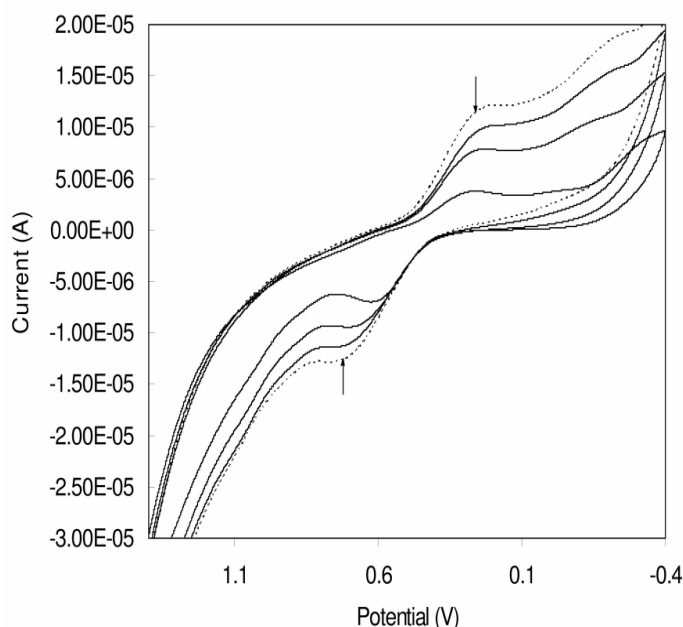


**Fig. S5.** Cyclic voltammogram in DMF:buffer [mixture 50 mM Tris–HCl/NaCl buffer (pH, 7.2)] (1:2) solution of **1** (Scan rate = 0.08 Vs<sup>-1</sup>) with incremental addition of CT DNA. 0.05M n-Bu<sub>4</sub>NClO<sub>4</sub> as supporting electrolyte and the arrow mark indicates the current changes upon increasing DNA concentrations.

**Table 4**

Electrochemical parameters of interaction of DNA with copper complexes

Complexes	$\Delta E_p$ (V)		$E_{1/2}$ (V)		Decrease of $i_{pc}$ (%)	$i_{pa}/i_{pc}$		$K_+/K_{2+}$
	Free	Bound	Free	Bound		Free	Bound	
<b>1</b>	0.139	0.130	0.515	0.498	18	0.92	0.85	0.84
<b>3</b>	0.189	0.181	0.343	0.331	13	0.96	0.87	0.89

In the absence of CT DNA, the redox couple anodic peak appeared at  $-0.294$  to  $-0.342$  V. Incremental addition of DNA to the Zn(II) complexes showed (Table 5) a decrease in the current intensity and a negative shift of the oxidation peak potential. The resulting changes in the current and potential demonstrate that there is an interaction between Zn(II) and DNA.

**Table 5**

Electrochemical parameters for the interaction of DNA with zinc complexes

Complexes	Ep (V)		$i_{pc}$ ( $\mu A$ )		$K_d \times 10^{-10}$ ( $molL^{-1}$ )
	Free	Bound	Free	Bound	
<b>2</b>	0.748	0.736	0.74	0.30	1.3
<b>4</b>	0.698	0.685	0.65	0.42	1.4

Cyclic voltammogram of the complex 4 in the absence and in the presence of varying amount of [DNA] is shown in Fig. S6 (supplementary material). An increase in the concentration of DNA caused a negative potential shift along with a significant decrease of the current intensity. The shift in the potential is related to the ratio of the binding constants by the following equation:

$$E_b^{\circ} - E_f^{\circ} = 0.059 \log(K_+/K_{2+})$$

where  $E_f^{\circ}$  and  $E_b^{\circ}$  are the formal potentials of the, Cu(II)/Cu(I) couple in the free and bound forms, respectively. The ratio of the binding constants ( $K_+/K_{2+}$ ) for DNA binding of the synthesized complexes were calculated and found to be less than one. The above electrochemical experimental results indicate the preferential stabilization of Cu(II) form on binding to DNA over other forms.

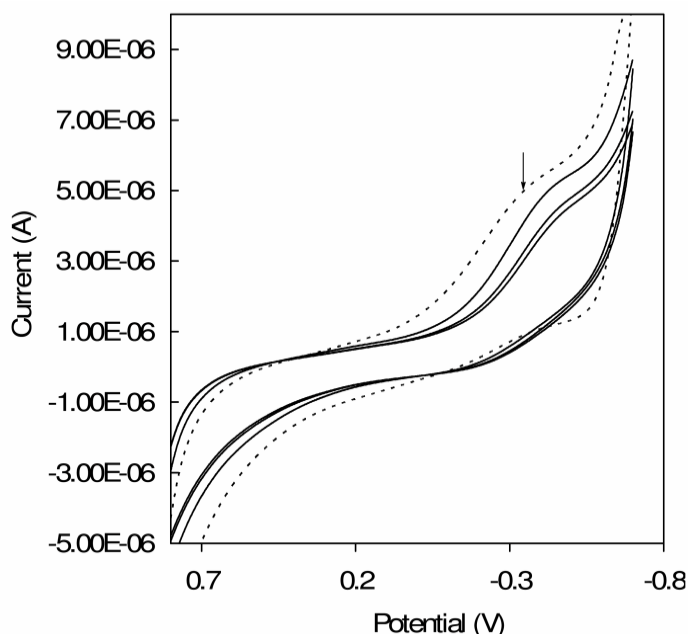
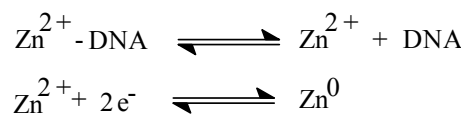


**Fig. S6.** Cyclic voltammogram in DMF:buffer [mixture 50 mM Tris-HCl/NaCl buffer (pH, 7.2)] (1:2) solution of 4 (Scan rate =  $0.08 \text{ Vs}^{-1}$ ) with incremental addition of CT DNA. 0.05M  $n\text{-Bu}_4\text{NClO}_4$  as supporting electrolyte and the arrow mark indicates the current changes upon increasing DNA concentrations.

Differential pulse voltammogram of the presented Zn(II) complex showed a negative potential shift along with a significant decrease of current intensity during the addition of increasing amounts of DNA. This indicates that the zinc ion stabilizes the duplex (GC pairs) by intercalation. Hence, for the complex of the electroactive species [Zn(II)] with DNA, the electrochemical reduction reaction can be divided into two steps



The dissociation constant ( $K_d$ ) of the Zn(II)-DNA complex was obtained using the following equation:

$$i_p^2 = \frac{K_d}{[\text{DNA}]} (i_{p0}^2 - i_p^2) + i_{p0}^2 - [\text{DNA}]$$

where  $K_d$  is dissociation constant of the complex Zn(II)-DNA,  $i_{p0}^2$  and  $i_p^2$  are reduction current of Zn(II) in the absence and presence of DNA respectively. The low dissociation constant values ( $10^{-10}$  order) of Zn(II) ions were indispensable for structural stability of complexes Zn(II)-DNA which participate in the replication, degradation and translation of genetic material of all species.

### 3.7.3. DNA binding analysis using viscosity measurement

To throw further light on the DNA binding mode, viscosity measurements which regarded as the least ambiguous and the most critical test of a DNA binding model in solution and provides stronger arguments for intercalative DNA binding mode, has been undertaken [31,32]. A classical intercalation model results in the lengthening of the DNA helix because base pairs become separated to accommodate the binding ligand, leading to an increase in the viscosity of CT-DNA. In contrast, a partial and/or non-classical intercalation of ligand could bend (or kink) the DNA helix, reducing its effective length and, concomitantly, its viscosity [33,34]. The effect on the CT-DNA shown in Fig.4 reveals that the relative viscosity of DNA increased steadily following the order  $1 > 3 > 2 > 4$ , with an increasing amount of the above compounds. The increased degree of viscosity may depend on the affinity of the compounds to DNA.

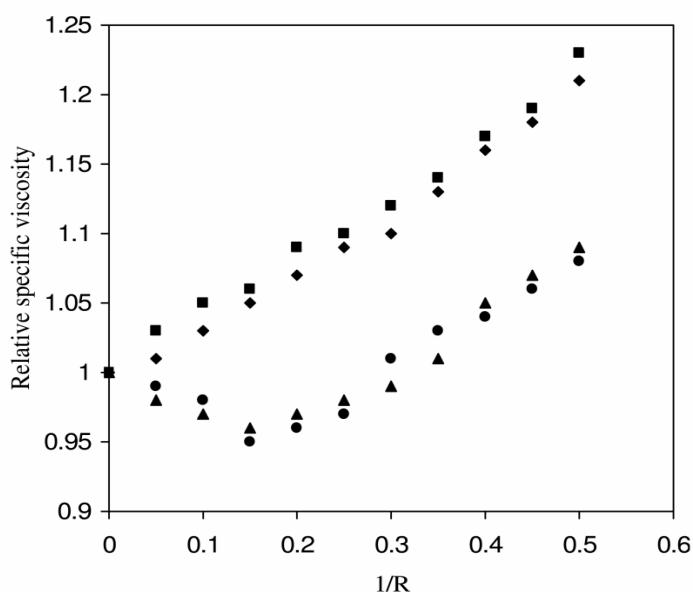


**Fig. 4.** Effect of increasing concentrations of complexes of **1** (■), **2** (▲), **3** (◆) and **4** (●) on the relative viscosity of CT DNA at  $25.0 \pm 0.1$  °C.  $[\text{DNA}] = 10 \mu\text{M}$ ,  $R = [\text{complex}] / [\text{DNA}]$

## 3.8. Pharmacological results and discussion

The minimum inhibitory concentration (MIC) values of the compounds against the growth of microorganisms are summarized in Table 6 and Table 7. A comparative study of MIC values of the Schiff base and its complexes indicate that, generally, the metal complexes have a better activity than the free ligand. This is probably due to the greater lipophilic nature of the complexes. Such increased activity of the metal chelates can be explained on the basis of chelating theory [35]. On chelating, the polarity of the metal ion will be reduced to a greater extent due to the overlap of the ligand orbital and partial sharing of positive charge of the metal ion with donor groups. Further, it increases the delocalization of  $\pi$ -electrons over the whole chelate ring and enhances the lipophilicity of the complex. This increased lipophilicity enhances the penetration of the complexes into lipid membrane and blocks the metal binding sites on enzymes of micro-organisms.

**Table 6**  
Antibacterial activity of synthesized compounds

Compound	Minimum inhibitory concentration (MIC) ( $\times 10^4 \mu\text{M}$ )			
	<i>Staphylococcus aureus</i>	<i>Bacillus subtilis</i>	<i>Escherichia coli</i>	<i>Salmonella typhi</i>
L	19.8	20.1	17.0	18.3
<b>1</b>	1.9	2.9	1.6	2.5
<b>2</b>	1.8	2.7	1.5	2.2
<b>3</b>	2.0	2.8	1.7	2.4
<b>4</b>	1.9	2.6	1.4	2.1
Streptomycin	1.7	2.5	1.3	2.0

**Table 7**  
Antifungal activity of synthesized compounds

Compound	Minimum inhibitory concentration (MIC) ( $\times 10^4 \mu\text{M}$ )			
	<i>Staphylococcus aureus</i>	<i>Bacillus subtilis</i>	<i>Escherichia coli</i>	<i>Salmonella typhi</i>
L	19.8	20.1	17.0	18.3
<b>1</b>	1.9	2.9	1.6	2.5
<b>2</b>	1.8	2.7	1.5	2.2
<b>3</b>	2.0	2.8	1.7	2.4
<b>4</b>	1.9	2.6	1.4	2.1
Streptomycin	1.7	2.5	1.3	2.0

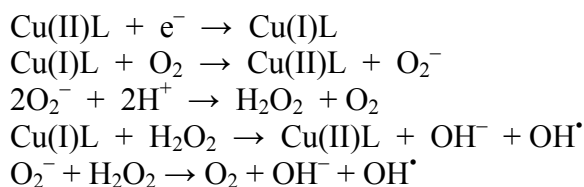
In the present study, all chemically synthesized compounds were evaluated against two Gram-positive, two Gram-negative bacteria and four fungi. All the compounds possessed good antibacterial activity against Gram-negative bacteria (*Escherichia coli*). However all the compounds were not sufficient effective against Gram-positive bacteria (*Bacillus subtilis* and *Staphylococcus aureus*).

It was demonstrated that the metal complexes showed a higher effect on *Escherichia coli* than on *Bacillus subtilis* and this difference could be due to the Gram-status. It is known that the membrane of Gram-negative bacteria is surrounded by an outer membrane containing

lipopolysaccharides. The newly synthesized Schiff bases seem to be able to combine with the lipophilic layer in order to enhance the membrane permeability of the Gram-negative bacteria. The lipid membrane surrounding the cell favors the passage of only lipid soluble materials; thus the lipophilicity is an important factor that controls the antimicrobial activity. Also the increase in lipophilicity enhances the penetration of Schiff base into the lipid membranes and thus restricts further growth of the organism [36]. This could be explained by the charge transfer interaction between the Schiff base molecules and the lipopolysaccharide molecules which leads to the loss of permeability barrier activity of the membrane. It is found that all the synthesized metal complexes show strong antimicrobial activity at lower concentration when compared to earlier reported literature [37, 38].

### 3.8.1. Chemical nuclease activity

The chemical nuclease activity of the complexes 1–4 (25  $\mu\text{M}$ ) was investigated by gel electrophoresis using hydrogen peroxide (50  $\mu\text{M}$ ) as an oxidising agent. At micro-molar concentrations, for 2 h incubation period, the ligand exhibits no significant cleavage activity in the absence or presence of oxidant ( $\text{H}_2\text{O}_2$ ). The nuclease activity of the complexes is also investigated in the presence and absence of an oxidant like  $\text{H}_2\text{O}_2$ . From Fig. S7 (supplementary material), it is evident that the copper complexes cleave DNA more efficiently in the presence of an oxidant. This may be attributed to the formation of hydroxyl free radicals. The production of a hydroxyl radical due to the reaction between the metal complex and oxidant may be explained as shown below:



These OH free radicals participate in the oxidation of the deoxyribose moiety, followed by hydrolytic cleavage of the sugar phosphate backbone. The more pronounced nuclease activity of these adducts in the presence of oxidant as compared to the parent complexes [Fig. S7 (supplementary material), lanes 3-8] may be due to the increased production of hydroxyl radicals. Even in the absence of oxidant, the complexes exhibit significant DNA cleavage activity (e.g. lanes 4 and 6). This may be due to the ability of the complexes to associate with DNA, facilitated by hydrophobic interaction leading to fair nucleolytic cleavage. It may be due to the inability of zinc complexes to produce hydroxyl radical continuously. Hence, zinc complexes cleave DNA only *via* hydrolytic path way [39] and not for oxidant path way. Redox active copper complexes cleave DNA by an oxidative path way. It is also an example where chemically or electrochemically generated metal in high oxidation state can act as an oxidant in the presence of a  $\text{H}_2\text{O}_2$ . Copper complexes usually do not mediate nucleobase oxidation, but are responsible for direct strand scission by hydrogen atom abstraction from the deoxyribose moiety. Similar results have been reported in other cases [40]. The results indicate the importance of the metal in the complex for observing the chemical nuclease activity.

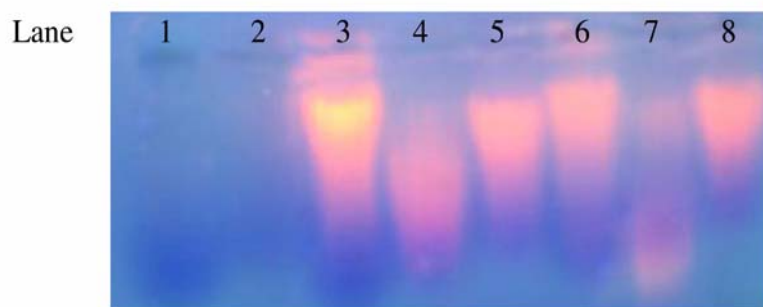


**Fig. S7.** Gel electrophoresis diagram showing the cleavage of pBR322 DNA (0.10 µg) by the synthesized complexes (25 µM): Lane 1: DNA alone; Lane 2: DNA + Ligand; Lane 3: DNA + 1 + H<sub>2</sub>O<sub>2</sub>; Lane 4: DNA + 1; Lane 5: DNA + 2 + H<sub>2</sub>O<sub>2</sub>; Lane 6: DNA + 3; Lane 7: DNA + 3 + H<sub>2</sub>O<sub>2</sub>; Lane 8: DNA + 4.

#### 4. Conclusions

Based on the above observations of the elemental analysis, molar conductivity, UV-vis, magnetic, IR and <sup>1</sup>H NMR spectral data, it is possible to determine the type of coordination of the ligand in their metal complexes. The correlation of the experimental data allows assigning a square-planar geometry for the complexes 1 and 2, an octahedral geometry for the complexes 3 and 4. The better binding properties of the complexes should be attributed to the good coplanarity of the ligand after coordination with metal ions. Gel electrophoresis experiment suggests that the complex cleaves DNA in the presence of hydrogen peroxide. Cu(II) and Zn(II) complexes have been synthesized and their abilities to induce oxidatively generated DNA damage are compared. The metal complexes have more biological activity than the free ligand.

#### Acknowledgment

The authors express their sincere thanks to the College Managing Board, Principal and Head of the Department of Chemistry, VHNSN College for providing necessary research facilities and financial support. Instrumental facilities provided by Sophisticated Analytical Instrument Facility (SAIF) IIT Bombay and CDRI Lucknow are gratefully acknowledged.

#### References

- [1] D.M.C. Maria, Ribeiro da Silva, M.G. Jorge, L.R.S. Ana, C.F.C. Paula, Bernd Schroder, A.V. Manual, *J. Mol. Catal. A: Chem.* 224 (2004) 207-212.
- [2] C. Spinu, A. Kriza, *Acta. Chem. Slov.* 47 (2000) 179-185.
- [3] D.M. Boghaei, M. Gharagozlou, *Spectrochim. Acta Part A* 67 (2007) 944-949.
- [4] N. Raman, K. Pothiraj, T. Baskaran, *J. Mol. Struct.* 1000 (2011) 135-144.
- [5] D. Sattari, E. Alipour, S. Shriani, J. Amighian, *J. Inorg. Biochem.* 45 (1992) 115-122.
- [6] A. Sreedhara, J.A. Cowan, *J. Biol. Inorg. Chem.* 6, (2001) 337-347.
- [7] Y. Lu, *Chem. Eur. J.* 8 (2002) 4588-4596.
- [8] N. Sträter, W.N. Lipscomb, T. Klabunde, B. Krebs, *Angew. Chem. Int. Ed. Engl.* 35 (1996) 2024-2055.
- [9] T.M. Aminabhavi, N.S. Biradar, S.B. Patil, V.L. Roddabasanagoudar, W.E. Rudzinski, *Inorg. Chim. Acta* 107 (1985) 231-234.
- [10] Vogel A Text Book of Quantitative Inorganic Analysis (3rd ed.). ELBS, Longman, London, 1969.
- [11] Y.Z. Cai, Q. Luo, M. Sun, H. Corke, *Life Sci.* 74 (2004) 2157-2184.
- [12] K.E. Heim, A.R. Tagliaferro, D.J. Bobilya, *J. Nutr. Biochem.* 13 (2002) 572-584.
- [13] L.G. Van Waasbergen, I. Fajdetic, M. Fianchini, H.V. Rasika dias, *J. Inorg. Biochem.* 101 (2007) 1180-1183.
- [14] J. Bernadou, G. Pratviel, F. Bennis, M. Girardet, B. Meunier, *Biochemistry*, 28 (1989) 7268-7275.

- [15] T.C. Michael, R. Marisol, J.B. Allen, *J. Am. Chem. Soc.* 111 (1989) 8901-8911.
- [16] M.S. Ameerunisha Begum, S. Saha, M. Nethaji, A.R. Chakravarty, *J. Inorg. Biochem.* 104 (2010) 477-484.
- [17] N. Raman, R. Jeyamurugan, A. Sakthivel, L. Mitu, *Spectrochim. Acta part A* 75 (2010) 88-97.
- [18] M.S. Sujamol, C.J. Athira, Y. Sindhu, K. Mohanan, *Spectrochim. Acta part A* 75 (2010) 106-112.
- [19] E. Tas, M. Aslanoglu, A. Kilic, Z. Kara, *J. Coord. Chem.* 59 (2006) 861-872.
- [20] M. Odabasoglu, F. Arslan, H. Olmez, O. Buyukgungor, *Dyes Pigm.* 75 (2007) 507-515.
- [21] Z. Chen, Y. Wu, D. Gu, F. Gan, *Spectrochim. Acta part A* 68 (2007) 918-926.
- [22] A. Biswas, M.G.B. Drew, A. Ghosh, *Polyhedron* 29 (2010) 1029-1034.
- [23] N. Raman, A. Selvan, *J. Coord. Chem.* 64 (2011) 534-553.
- [24] F.A. Cotton, G. Wilkinson, *Advanced Inorganic Chemistry. A Comprehensive Text* (4th ed.) John Wiley and Sons, New York, 1986.
- [25] B.J. Hathaway, D.E. Billing, *Coord. Chem. Rev.* 5 (1970) 143-207.
- [26] G. Speir, J. Csihony, A.M. Whalen and C.G. Pierpont, *Inorg. Chem.* 35 (1996) 3519-3524.
- [27] J.K. Barton, A.T. Danishefsky, J.M. Goldberg, *J. Am. Chem. Soc.* 106 (1984) 2172-2176.
- [28] N. Raman, A. Sakthivel, R. Jeyamurugan, *J. Coord. Chem.* 62 (2009) 3969-3985.
- [29] N. Raman, R. Jeyamurugan, R Usha Rani, T. Baskaran, L. Mitu, *J. Coord. Chem.* 63 (2010) 1629-1644.
- [30] L.F. Tan, X.H. Liu, H. Chao and L.N. Ji, *J. Inorg. Biochem.* 101 (2007) 56-63.
- [31] F. Arjmand, M. Aziz, *Eur. J. Med. Chem.* 44 (2009) 834-844.
- [32] S. Mahadevan, M. Palaniandavar, *Inorg. Chem.* 37 (1998) 693-700.
- [33] A.B. Tossi, J.M. Kelly, *Photochem. Photobiol.* 9 (1989) 545-556.
- [34] S. Satyanarayana, J.C. Dabrowiak, J.B. Chaires, *Biochemistry*, 31 (1992) 9319-9324.
- [35] B.D. Wang, Z.Y. Yang, D.W. Zhang, Y. Wang, *Spectrochim. Acta part A* 63 (2006) 213-219.
- [36] J.W. Searl, R.C. Smith, S.J. Wyard, *Proc. Phys. Soc.* 78 (1961) 1174-1176.
- [37] P.V. Rao, A.V. Narasaiah, *Indian J. Chem. A* 42 (2003) 1896-1899.
- [38] N. Raman, A. Selvan, P. Manisankar, *Spectrochim. Acta part A* 76 (2010) 161-173.
- [39] N. Raman, A. Sakthivel, R. Jeyamurugan, *J. Coord. Chem.* 63 (2010) 1080-1096.
- [40] N. Raman, A. Sakthivel, K. Rajasekaran, *J. Coord. Chem.* 62 (2009) 1661-1676.